Closed-Loop Single-Beacon Passive Acoustic Navigation for Low-Cost Autonomous Underwater Vehicles

Nicholas R. Rypkema[1], Erin M. Fischell[2] and Henrik Schmidt[1]

***Abstract*— Accurate localization is critical for a robotic vehicle to navigate autonomously. Conventional autonomous underwater vehicles (AUVs) typically rely on an inertial navigation system (INS) aided by a Doppler velocity log (DVL) in order to reduce the rate of positional error growth of dead-reckoning to a level suitable for reliable navigation underwater. The size, cost, and power requirements of these systems result in vehicles that are prohibitively large and expensive for multi-AUV operations. In this work we present the first results of closed-loop experiments using a miniature, low-cost SandShark AUV and a custom-designed, inexpensive acoustic system first described in our previous work. Results are validated using an independent LBL system, and indicate that our approach is suitably accurate to enable the self-localization of such AUVs without the use of an expensive DVL-aided INS. Self-localization is performed by obtaining acoustic range and angle measurements from the AUV to a single acoustic beacon using a vehicle-mounted passive hydrophone receiver-array, and fusing these measurements using a particle filter. A critical aspect of our approach that allows for real-time, closed-loop operation is the close coupling of conventional phased-array beamforming and particle filtering – this implementation detail reduces the computational complexity associated with our previously described two-stage beamforming plus particle filtering process, and consequently also enables an increase in particle count and an improvement in navigational accuracy. Experimental results are provided for two cases: first, absolute navigation in the case where the beacon is fixed at a known position; and second, relative navigation with a moving beacon, a novel operating paradigm for AUVs which promises to enable multi-AUV operations while maintaining bounded navigation error.**

I. Introduction

Advances in the navigational reliability of autonomous underwater vehicles (AUVs) has seen the widespread acceptance and use of these vehicles for a variety of oceanographic, industry, and defense applications. A long-held goal of AUV research has been the coordinated use of multiple vehicles to enable novel applications, such as the effective sampling of highly dynamic ocean processes, or coherent acoustic processing over many AUVs. Unfortunately, navigational reliability has been achieved through the development and use of a sophisticated sensor system, namely the Doppler velocity log (DVL)-aided inertial navigation system (INS) [2], [3], which drives up vehicle price, power use, and size. As a result, AUV deployments tend to be unwieldy and risk-averse, and multi-vehicle operations remain out of reach for most researchers. However, the emergence of a new class of very low-cost, miniature AUV such as the SandShark [4] holds the promise of once again facilitating multi-AUV research. Unfortunately, the absence of a DVL-aided INS on these vehicles results in rapid unbounded accumulation of dead-reckoning navigation error. This work addresses this problem with an acoustic system that bounds this error growth and is inexpensive, simple to use, and which easily scales with the addition of more vehicles. The key characteristics of this system are: 1. the use of a single beacon that periodically transmits an acoustic signal to the vehicle, reducing cost and increasing ease of deployment; and 2. the completely passive synchronous reception of the acoustic signal by an AUV-mounted ultra-short baseline (USBL) array, which reduces power use and cost, and enables multiple vehicles to localize using just a single beacon.

Fig. 1: The prototype miniature SandShark AUV from Bluefin Robotics, outfitted with our passive acoustic navigation payload. Unlike conventional AUVs, the vehicle has no DVL and uses a low-grade MEMS IMU.

II. Related Work

Although significant advances have been made in geophysical positioning techniques for AUVs, including terrain relative [5] and sonar-based [6], [7] localization, acoustic approaches remain the most robust and reliable across changing environments. However, classical long, short, and ultra-short baseline (L/S/USBL) acoustic positioning systems suffer from limitations in price, cost of communications, ease of use, scalability, or some combination thereof [1].

LBL systems use widely spaced, fixed transponders which respond to vehicle ranging requests, allowing AUV self-localization via trilateration and two-way travel-time (TWTT) ranging. Early work by Newman and Leonard [8], Vaganay et al. [9] and Curcio et al. [10] sought to improve ease-of-use of LBL systems, by removing the need to manually geolocate the transponders either through simultaneous localization and mapping (SLAM) techniques, or by using high navigation accuracy vehicles as mobile transponders in a moving LBL approach. Unfortunately, the use of TWTT in

[1]N. R. Rypkema is with the Electrical Engineering and Computer Science Department, and H. Schmidt is with the Mechanical Engineering Department, Massachusetts Institute of Technology, Cambridge, MA 02139, USA, {rypkema, henrik}@mit.edu

[2]E. M. Fischell is with the Applied Ocean Physics and Engineering Department, Woods Hole Oceanographic Institution, Woods Hole, MA 02543, USA, efischell@whoi.edu

these approaches means that each AUV must carry an active acoustic system to transmit ranging requests, increasing price and communications cost. In addition, this severely restricts scalability, since the acoustic channel must be time or frequency shared across multiple AUVs and transponders.

To overcome these issues in scalability, Singh et al. [11] and others proposed the use of one-way travel-time (OWTT) ranging through vehicle-transponder clock synchronization. Recent work by Melo and Matos [12] experimentally demonstrated a OWTT LBL system, in which multiple AUV surrogates were localized using an extended Kalman filter (EKF) and OWTT ranges to fixed beacons.

The disadvantage of LBL systems is that they always require multiple transponders. This adds cost, and carries a penalty in terms of setup time or communications depending on whether the transponders are fixed or mobile. In contrast, USBL and inverted USBL (iUSBL) systems are able to provide a full navigation fix using a single source. A transponder containing an array of transducers is used to calculate range and angle to the source using TWTT and phase-differencing. Recent work by Hodgkinson et al. [13] and Morgado at al. [14] has demonstrated AUV self-localization using iUSBL. Again, scalability remains a problem due to TWTT.

An interesting approach that addresses many of these limitations in communications cost, ease of use, and scalability was first outlined by Eustice et al. [15], and improved upon by Webster et al. [16], in which OWTT range measurements to a single beacon are accrued over time and fused with dead-reckoning to bound positional error growth. More recently, Claus et al. [17] have demonstrated closed-loop results of this approach. Unfortunately, these systems require a DVL-aided INS to prevent dead-reckoning error from growing more quickly than can be reduced by acoustic ranging. Additionally, the vehicle is required to receive multiple range measurements from a variety of relative bearings in order to attain a suitably unambiguous positional fix.

These previous approaches have successfully overcome some, but not all, of the limitations of classical acoustic positioning systems. In contrast, the work we present here addresses each of these limitations by combining the advantages of OWTT (scalability due to passive reception) and an iUSBL receiver (full navigation fix via triangulation of range and angle). We previously demonstrated the feasibility of this approach using *offline* processing of acoustic measurements in [18] and [19]. Our system operates using a single acoustic beacon that periodically emits a known waveform; time-synchronization between this beacon and the vehicle allows for synchronous passive reception of this signal by an AUV-mounted USBL hydrophone array; finally, vehicle attitude combined with matched filtering and beamforming for range and angle estimation to the beacon provides an instantaneous estimate of relative vehicle position. In this work we detail a critical improvement in our approach that enables *real-time*, *online* operation on a low-cost, embedded computer – this is achieved by closely coupling phased-array beamforming and particle filtering. Our system also enables a novel operating paradigm for AUVs that is not possible with range-only

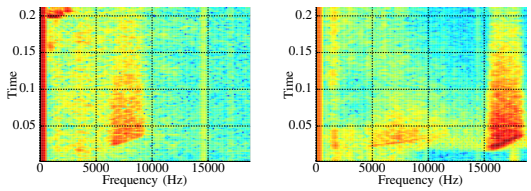

Fig. 2: Example time-frequency in-water spectrograms of LFM signals broadcast by our custom acoustic beacon. *Left*: 20 ms, 7–9 kHz up-chirp. *Right*: 20 ms, 16–18 kHz up-chirp.

approaches – navigation relative to a *moving* beacon whose absolute position is opaque to the vehicle. By constraining vehicle movement to an area local to the beacon, this paradigm enables the AUV to bound the range-dependent positional error associated with USBL systems, facilitating AUV deployments over large spatial length scales.

This paper details our system hardware and software, and presents the first results of closed-loop experiments undertaken using a miniature, low-cost Bluefin Robotics SandShark AUV outfitted with our acoustic navigation payload (Fig. 1). The single-beacon, acoustically passive nature of our system has led us to describe the system as single-beacon, passive inverted ultra-short baseline (piUSBL) positioning.

III. Single Beacon Acoustic Transmitter

The system makes use of a single custom-made acoustic beacon consisting entirely of commercial-off-the-shelf components. The beacon does not communicate with the vehicle, but instead periodically broadcasts a user-defined acoustic signal at a rate of 1 Hz.

The beacon is comprised of three principal components. The first is a GPS receiver used to provide precise time synchronization to the pulse-per-second (PPS) signal of a GPS satellite. The PPS signal is input into a digital pin on an Arduino Uno with Wave Shield, which allows it to detect the onset of each second – this in turn triggers the Wave Shield to output a locally stored user-defined acoustic signal. Finally, this signal is broadcast into the water through a Lubell amplifier and underwater speaker.

The use of an Arduino microcontroller is critical to ensure extremely consistent ($\leq$ 1 ms jitter) periodic transmission of the acoustic signal. The customizable nature of this beacon allows us to broadcast a variety of different signals as shown in figure 2, enabled by the wideband (200 Hz – 23 kHz) frequency response of the Lubell underwater speaker.

IV. Passive Inverted Ultra-Short Baseline (piUSBL) Receiver

A. Receiver Hardware

The passive acoustic receiver is implemented as a payload on a prototype Bluefin SandShark miniature AUV, making up the front $2/3$'s of the vehicle pictured in figure 1. The rear $1/3$ of the vehicle is the standard SandShark platform, which consists of a single magnetically-coupled propeller and motor, two stepper motors for elevator and rudder fin control, a pressure sensor for depth, a GPS and WiFi receiver, and a low-grade 9-axis MEMS IMU. Attitude and speed data is filtered from IMU and prop RPM and made available to

the payload, which in turn uses this information to command AUV speed, heading, and depth using the MOOS-IvP [20] autonomy framework. The lack of DVL and high-grade IMU allows for the vehicle to be inexpensive and small, with a 12.4 cm diameter and a total length of about 115 cm.

The piUSBL acoustic receiver has five integral hardware components. The first is a nose-mounted tetrahedral USBL array with a spacing of 4.5 cm, consisting of four hydrophones used to detect the broadcast acoustic signal which then passes through a custom analog amplification board. Analog-to-digital conversion is performed using a digital acquisition (DAQ) device, and this digital signal is processed using a Raspberry Pi 3 embedded computer using our online navigation algorithm. The fifth and most critical component of the system is a GPS disciplined oscillator containing a SA.45 chip-scale atomic clock (CSAC), providing the payload with a highly precise GPS-synchronized PPS signal. The CSAC triggers the DAQ at the onset of each second, allowing the receiver to record hydrophone measurements in sync with beacon broadcasts, effectively enabling OWTT ranging to the acoustic beacon. The DAQ is set to record 8000 samples every second at a sampling rate of 37.5 kS/s – assuming a sound speed in freshwater of 1481 m/s, this gives our system an effective range of about 316 m ($r_{max} = \frac{c}{Fs} \cdot n = \frac{1481 \text{ m/s}}{37500 \text{ S/s}} \cdot 8000 \text{ S} \approx 316 \text{ m}$).

B. Range Estimation

The AUV estimates range to the acoustic beacon through the use of matched filtering, following the same approach as in our previous work [18, Sec. II-B]. The time-domain signals on each hydrophone $x_i[n]$ are essentially cross-correlated with a template of the broadcast signal $h[n]$:

$$y_i[n] = \sum_{k=0}^{N-1} h[n-k]x_i[k] \tag{1}$$

If the standard deviation of the arg-maximums from all four resulting signals is below a specified threshold, then the array measurement is deemed valid (invalid measurements typically occur when the vehicle acoustically obstructs the array). The four signals are then combined by taking the sum of the product of all unique signal combinations:

$$y'[n] = \sum_{i,j=1}^{4} |y_i[n]||y_j[n]| \qquad i \neq j \tag{2}$$

Finally, this combined output is normalized and converted from the time-domain to range-domain by multiplying by the speed of sound in freshwater, resulting in a range signal whose *argmax* provides an instantaneous estimate of distance between the AUV and the acoustic beacon.

C. Azimuth and Inclination Estimation

An estimate of the azimuth and inclination from the AUV to the beacon in the body-fixed frame of the vehicle is achieved using conventional phased-array beamforming (CBF) [21]. Under a far-field assumption, the broadcast signal incident onto the hydrophone array can be assumed to be planar; for a given azimuth-inclination combination (look-angle), the geometry of the array and the look-angle direction

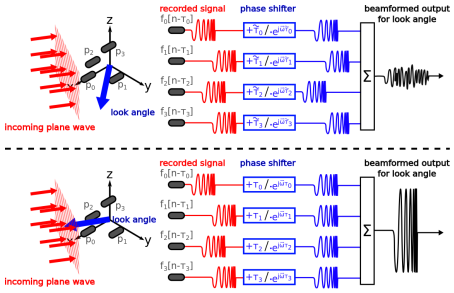

Fig. 3: Conceptual illustration of conventional phased-array beamforming. *Top*: beamformer power output is small when the look-angle is pointing away from the incoming signal. *Bottom*: received signals sum constructively when the look-angle is correct, resulting in high beamformer power output.

can then be used to apply a time-delay (phase-shifts) to the received signal. Thus, the aim is to steer the beamformer over a set of candidate look-angles, and to select the azimuth and inclination that results in the maximum beamformer output power; this occurs when the look-angle points in the direction of the incoming plane wave and the phase-shifted signals add constructively, as illustrated in figure 3.

Given the position $\vec{p_i}$ of each array element relative to an arbitrary origin, the time delay between element i and the origin of an incident plane wave from a given look-angle is:

$$\tau_i = -\frac{\vec{u}^T \vec{p_i}}{c} \qquad where: \ \vec{u} = \begin{bmatrix} \sin(\theta)\cos(\phi) \\ \sin(\theta)\sin(\phi) \\ \cos(\theta) \end{bmatrix} \tag{3}$$

where c is speed-of-sound in water, and ϕ and θ are azimuth and inclination respectively. Applying this time-delay to the signal f_i received by element i is equivalent to applying phase-shifts in the frequency domain:

$$f_i[n - \tau_i] \overset{DFT/IDFT}{\rightleftharpoons} F_i[\omega] \cdot e^{-j\vec{\omega}\tau_i} \tag{4}$$

where $\vec{\omega}$ is the vector of frequencies of the n-point DFT. Beamforming negates these geometrically-induced time delays using a spatial filter $H_i[\omega;\theta,\phi]$ for each element that applies opposing phase-shifts, and sums over all elements:

$$Y[\omega;\theta,\phi] = \sum_{i=1}^{4} H_i[\omega;\theta,\phi] \cdot F_i[\omega] \tag{5}$$
$$where: \ H_i[\omega;\theta,\phi] = e^{j\vec{\omega}\tau_i}$$

The beamformer frequency-averaged output power is then:

$$|\widetilde{Y}[\theta,\phi]|^2 = \frac{1}{n}\sum_{n} |Y[\omega_n;\theta,\phi]|^2 \tag{6}$$

The previously described matched filter is applied to the received signals to enhance detection, and the Chirp Z-transform is used rather than a full DFT to reduce n without loss of resolution in the frequency range of interest.

When the look-angle is pointing toward the acoustic beacon, the output power is large. By steering the look-angle over a set of candidates and searching for the largest response, the likeliest angle to the source can be found, providing an instantaneous estimate of the azimuth and inclination between the AUV and the beacon:

$$(\widetilde{\theta},\widetilde{\phi}) = \underset{\phi,\theta}{\text{argmax}} \ |\widetilde{Y}[\theta,\phi]|^2 \tag{7}$$

Unlike in our previous paper [18, Sec. II-C & II-D], in which we utilized a two-stage *offline* process of CBF acoustic processing followed by the sampling of this CBF output by a particle filter (PF) to fuse acoustic measurements and odometry, in this work we describe a method of closely coupling CBF with particle filtering, which we call the sequential Monte-Carlo beamformer. This tight integration is key in enabling *closed-loop*, online AUV navigation.

D. Sequential Monte-Carlo Beamformer

Performing an exhaustive search over a set of candidate look-angles is computationally expensive. In [18] we demonstrated real-time CBF using a gridded search-space of 4050 look-angles at about 1.25 Hz – this provided an angular resolution of 1.33° in azimuth and 12.00° in inclination. We also demonstrated through *offline* processing that a particle filter performed very well for localization, in part due to its ability to handle the multimodal nature of acoustic range and angle measurements (caused by undesirable effects such as multipath and interference). Unfortunately, real-time *online* integration of a PF with acoustic processing proved extremely challenging – it necessitated either a reduction in the angular resolution of the beamformer (thereby degrading our acoustic measurements), or a reduction in the number of particles in our filter (thereby degrading filter accuracy and exacerbating the degeneracy problem).

To overcome this computational bottleneck, we make use of a key insight: particle weights are updated and resampled in the domain of the CBF output, which is a grid of look-angles with values indicating the likeliest direction to the beacon; in this domain, the state of each particle is an azimuth-inclination combination, and thus they represent specific look-angles; the insight follows that we can simply beamform only at the look-angles represented by the set of particles in our filter, directly updating their weights in a single step. Therefore, instead of performing *only* real-time CBF with 4050 gridded *look-angles*, we can perform combined CBF and PF in real-time with 4050 *particles*. In effect, we make use of a certain complementarity between CBF and PF – the particles in the filter constrain the search space of beamforming to the area most likely to contain the maximum value (using the filter's motion model), and the beamformer provides the measurement update to each particle's weight. This concept is illustrated in figure 4.

1) Reference Frames and Transformations: Our sequential Monte-Carlo beamformer uses three reference frames, each using a right-hand coordinate system: the Forward-Port-Above body-fixed frame (bff), in which beamforming is performed (Eqs. 3–6); the vehicle-carried East-North-Up frame (vcf), whose origin is fixed to the vehicle's center of gravity; and the vehicle-carried East-North-Up *local-level* frame (llf), whose origin is also fixed to the vehicle's center of gravity, but in which both range and angle to the beacon are combined to estimate relative beacon position, and in which the filter motion update step is applied. A set of N particles with associated weights w_i^{llf} are stored in the

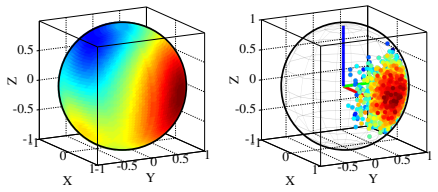

Fig. 4: Beamforming in the range-normalized AUV forward-port-up body-fixed frame. *Left*: Finding the likeliest angle to the beacon corresponds to an exhaustive search for the maximum power output over a grid of look-angles that covers the surface of the unit sphere. *Right*: The particles in the sequential Monte-Carlo beamformer use vehicle motion model to limit the search space to the area of the surface containing the global maximum. The left uses a total of 7200 look-angles, while the right uses only 1500.

llf and used to model the relative position of the acoustic beacon, with their states given by:

$$\vec{s}_i^{\,llf}(t) = \left[x_i^{llf}(t) y_i^{llf}(t) z_i^{llf}(t)\right]^T \tag{8}$$

Transforming between this set of combined range-angle llf particles, $\vec{s}^{\,llf}(t)$, and the separated range and angle particles in the range domain and the vcf requires us to perform a duplication of the set through a transformation denoted by R_{llf}^{vcf}. This is achieved by vector normalization and magnitude calculation respectively to get an angle-only vcf particle set $\vec{s}^{\,vcf}(t)$ and a range-only particle set $r(t)$:

$$(\vec{s}_i^{\,vcf}(t), r_i(t)) = R_{llf}^{vcf}(\vec{s}_i^{\,llf}(t)) \tag{9}$$

where:

$$r_i(t) = \|\vec{s}_i^{\,llf}(t)\| \tag{10}$$

$$\vec{s}_i^{\,vcf}(t) = \left[x_i^{vcf}(t) y_i^{vcf}(t) z_i^{vcf}(t)\right]^T = \frac{\vec{s}_i^{\,llf}(t)}{\|\vec{s}_i^{\,llf}(t)\|} \tag{11}$$

We denote the corresponding weights of these two sets as w_i^{bff} and w_i^r. We set them equal to w_i^{llf} during this transform:

$$(w_i^{bff}, w_i^r) = w_i^{llf} \tag{12}$$

The range-only particles r_i are now properly in the range domain for fusion with acoustic range measurements. However, the angle-only vcf particles $\vec{s}_i^{\,vcf}$ must still be transformed into the domain in which beamforming occurs, which is the bff. We see now why we denote the weights of the angle-only particles by w_i^{bff} – the vcf is only used as an intermediary frame between the llf and the bff. Transforming from the vcf to the bff is denoted by R_{vcf}^{bff}:

$$\vec{s}_i^{\,bff}(t) = \left[x_i^{bff}(t) y_i^{bff}(t) z_i^{bff}(t)\right]^T = R_{vcf}^{bff} \cdot \vec{s}_i^{\,vcf}(t) \tag{13}$$

$$\text{where:} \quad R_{vcf}^{bff} = R_z(\alpha) R_y(\beta) R_x(\gamma) \tag{14}$$

This is simply a rotational transformation using vehicle roll (γ)-pitch (β)-yaw (α) with the standard rotation matrices. The angle-only particles are now in the correct domain for beamforming. Transposing this rotation matrix provides the inverse transformation, denoted $R_{bff}^{vcf} = (R_{vcf}^{bff})^T$.

The inverse transformation from the separate range-only and angle-only particle sets back into the combined range-angle set $\vec{s}^{\,llf}(t)$ has a caveat: rather than multiplying each angle-only particle $\vec{s}_i^{\,vcf}$ and their associated weights w_i^{bff} by every range-only particle r_i and weight w_i^r (which would result in N^2 particles in $\vec{s}^{\,llf}(t)$), we instead sort $\vec{s}^{\,vcf}(t)$

and $r(t)$ in ascending order according to their respective weights w_i^{bff} and w_i^r; the inverse transform R_{vcf}^{llf} is then simply the element-wise multiplication of the sorted range-only and angle-only particle sets and their weights:

$$\vec{s}_i^{\,llf}(t) = R_{vcf}^{llf}(\vec{s}_i^{\,vcf}(t), r_i(t)) = \vec{s}_i^{\,vcf}(t) \cdot r_i(t) \quad (15)$$

$$w_i^{llf} = \frac{w_i^{bff} \cdot w_i^r}{\sum(w_i^{bff} \cdot w_i^r)} \quad (16)$$

This trick is not strictly correct, but allows us to maintain a constant number of N particles efficiently during duplication and recombination and performs well in practice. The reference frames used by the sequential Monte-Carlo beamformer and the transformations between each are shown in figure 5.

2) Initialization: Initialization of the filter is dependent on whether or not the acoustic beacon is fixed or mobile. In both cases all weights of the llf particles, $\vec{s}^{\,llf}(t)$, are initialized with equal weights, $w_i^{llf} = 1/N$. In addition, the particles are reinitialized whenever the vehicle surfaces.

Fixed beacon: If the beacon is fixed at a known position (x_{bcn}, y_{bcn}), the llf particles are initialized around the beacon's relative position using the vehicle's GPS position:

$$\vec{s}_i^{\,llf}(0) = \begin{bmatrix} (x_{bcn} - x_{\text{GPS}}(0) + \mathcal{N}(0, \sigma^2_{\text{GPS}})) \\ (y_{bcn} - y_{\text{GPS}}(0) + \mathcal{N}(0, \sigma^2_{\text{GPS}})) \\ \mathcal{N}(0, \sigma^2_{\text{GPS}}) \end{bmatrix} \quad (17)$$

Moving beacon: If the beacon is moving, the llf particles are instead initialized randomly with a uniform distribution within a spherical volume whose radius is equal to the maximum range of the system.

3) Motion Update: Once the vehicle dives and loses GPS reception, the particles are updated with a simple motion model that uses estimates of the AUV speed-over-ground (v_g) and yaw (α), provided to the payload by the SandShark platform. Since the platform lacks a DVL, speed-over-ground is calculated using prop RPM compensated by pitch. Because the filter is estimating the relative position of the beacon in the vehicle-centered llf, the direction opposite to vehicle travel is used to propagate the llf particles $\vec{s}_i^{\,llf}(t)$:

$$\vec{s}_i^{\,llf}(t) = \vec{s}_i^{\,llf}(t - \Delta t) - (v_g + \mathcal{N}(0, \sigma^2_{v_g}))\cdot \begin{bmatrix} \Delta t \cos(\alpha + \mathcal{N}(0, \sigma^2_\alpha)) \\ \Delta t \sin(\alpha + \mathcal{N}(0, \sigma^2_\alpha)) \\ 0 \end{bmatrix} - \begin{bmatrix} 0 \\ 0 \\ \Delta z \end{bmatrix} + \mathcal{N}(0, \sigma^2_{v_{bcn}}) \quad (18)$$

where Δz is the vehicle's change in depth from its pressure sensor, and Gaussian noise has been added to vehicle speed and yaw. The final term, $\mathcal{N}(0, \sigma^2_{v_{bcn}})$, is noise added to the particles that is representative of the speed of the beacon – if the beacon is fixed, its value is zero.

4) Measurement Updates: Whenever the system receives a valid acoustic measurement, the $\vec{s}^{\,llf}(t)$ local-level frame particle set is first transformed into duplicate sets of particles in the range-domain and body-fixed frame, using equations 9, 10, 11, 12, 13 and 14. This transformation gives us a range-only particle set, $r(t)$, and an angle-only particle set, $\vec{s}^{\,bff}(t)$, along with their associated weights w_i^r and w_i^{bff}.

The weights w_i^r of the particles r_i in the range domain are updated by multiplying against the range signal outputted from the matched filtering equations 1 and 2. Systematic resampling is then used to resample and reweight this set of range-only particles.

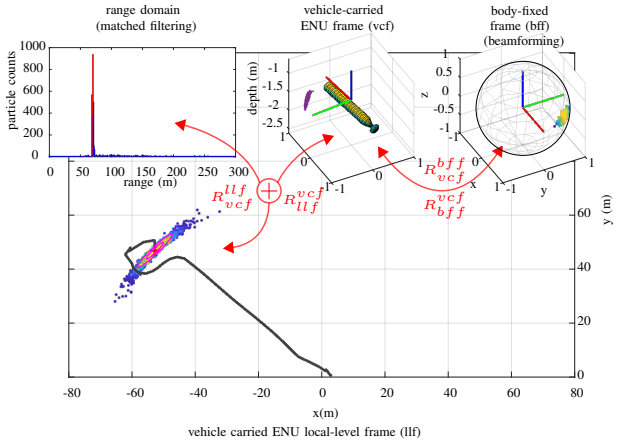

Fig. 5: Reference frames used by the sequential Monte-Carlo beamformer with 1500 particles. *Inset Left*: Range-domain with matched filter output in blue and histogram of range particle counts in red. *Inset Center*: Vehicle-carried ENU frame with vehicle attitude and angle particles shown in purple. *Inset Right*: Body-fixed frame with weighted angle particles shown in varying colors. *Main*: Vehicle-carried ENU local-level frame with combined range-angle weighted particles shown in varying colors.

The particles $\vec{s}_i^{\,bff}$ in the bff now represent look-angles at which to perform beamforming. The standard Cartesian-to-spherical transform provides the azimuths (ϕ) and inclinations (θ) at which to apply the set of beamforming equations, 3, 4, 5 and 6. Upon completion of beamforming at these look-angles, the weights w_i^{bff} of these angle-only particles are updated by multiplying against their corresponding beamformer output power, and systematic resampling is performed to obtain an updated particle set. The transform R_{bff}^{vcf} then places these particles into the vehicle-carried frame.

All that remains to be done is to transform these updated range-only and angle-only particle sets back into the local-level frame, which is done using the recombination equations 15 and 16. The filter loop then repeats.

5) Likelihood Estimation: To estimate the relative position of the acoustic beacon, we simply use the weighted mean of the particles $\vec{s}_i^{\,llf}$ in the local-level frame. When the beacon is fixed at a known position, absolute localization is possible by negating the relative beacon position and offsetting the result by the absolute coordinates of the beacon. For a moving beacon, the relative position enables the AUV to operate in a beacon-relative coordinate frame.

The localization performance of the sequential Monte-Carlo beamformer is comparable to the two-stage CBF plus PF approach from our previous work [18]. Its computational gain can be naively estimated as follows: assuming that the CBF processing time of a single look-angle is n ms, and the filter loop time of a single particle is m ms, given N look-angles and M particles, the total processing time for the two-stage CBF plus PF approach is about $((N \cdot n) + (M \cdot m))$ ms; conversely, for the sequential Monte-Carlo beamformer, the processing time is about $M \cdot (n + m) = ((M \cdot n) + (M \cdot m))$ ms; given the desired angular resolution of the beamformer, it is often the case that $M \ll N$, and therefore the net

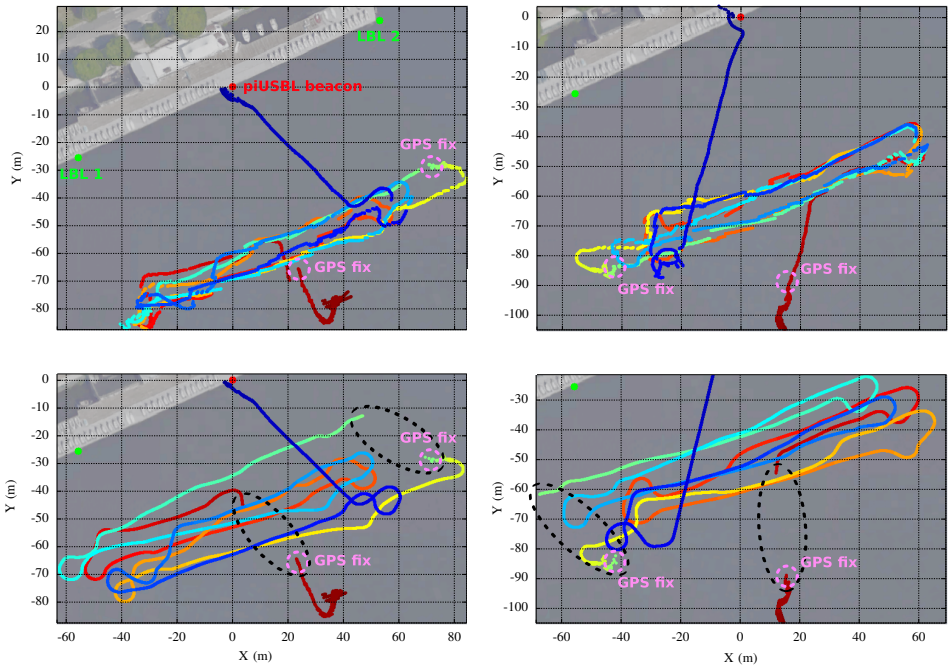

Fig. 6: . Closed-loop SandShark trajectory estimates - red dot indicates piUSBL beacon position, green dots indicate LBL transponder positions, pink dashed circles indicate AUV GPS surfacing positions. *Top Row*: piUSBL *closed-loop* trajectory estimates for run 1 (left) and run 2 (right). *Bottom Row*: Dead-reckoned *unused* trajectory estimates for run 1 (left) and run 2 (right). Colors of trajectories indicate elapsed mission time with *blue* indicating $t = 0s$ and *red* indicating $t \approx 1200s$. Dashed black ellipses indicate jump in dead-reckoned vehicle estimated position after receiving a surface GPS fix.

reduction in processing time is about $((N-M)\cdot n)$ ms. Filter performance in terms of both accuracy and computational efficiency is now directly proportional to a single parameter: the number of particles M.

V. Fixed Beacon Absolute Navigation

A. Field Experiments

To demonstrate single-beacon piUSBL absolute navigation, we carried out two closed-loop deployments of our SandShark AUV on a portion of the Charles River adjacent to the MIT sailing pavilion. Our custom acoustic beacon was set to broadcast a 20 ms, 16–18 kHz linear frequency modulated (LFM) up-chirp, and was affixed to the pavilion dock and submerged to a depth of approximately 1 m. The SandShark was programmed to run a mission to follow a racetrack parallel to the dock of 90 m length and 10 m width, at a depth of 2 m and a speed of 1 m/s. The mission length was set to 1200 s, with the vehicle instructed to surface for GPS approximately mid-way through the mission.

Since GPS is unavailable underwater, we also deployed two commercial Hydroid LBL transponders fastened to the pavilion at a depth of approximately 1 m, with the first transponder at position $(52.8, 23.8)$ m and the second at $(-55.6, -25.6)$ m relative to our custom acoustic beacon. The SandShark payload is equipped with a WHOI micro-modem that is not used for any purpose other than to query the LBL transponders at a rate of 0.2 Hz. This allows us to compare our solutions to the range values outputted by this independent system, providing a means for quantifying navigation accuracy. Note that the LBL system itself is subject to acoustic effects that result in range outliers. In order to remove these outliers, a simple constant velocity filter is employed - essentially, if the difference between subsequent LBL ranges is above the distance that can be achieved by the vehicle moving at maximum speed in that time delta, then that LBL measurement is discarded. This ensures that physically impossible LBL ranges are pruned from each dataset, but even so, some outliers still remain.

B. Results

Figure 6 displays the trajectories for both runs, estimated by our piUSBL system (top row) as well as naive dead-reckoning (DR, bottom row). The piUSBL estimates were used by the AUV for closed-loop navigation to follow the desired racetrack. Qualitative examination of these plots indicate that the piUSBL approach allows the vehicle to successfully self-localize, as evidenced by the minimal jumps in estimated position whenever the AUV surfaces and GPS reception is restored. In contrast, DR experiences jumps in position during run 1 of almost 30 m and 28 m during the mid-mission and end-mission surfacing events respectively; similarly, DR for run 2 has jumps of about 33 m and 36 m for these two surfacing events. A back-and-forth racetrack mission like this is expected to minimize dead-reckoning error, and demonstrates how quickly this error accumulates (at a rate of almost 3 m/min) in the absence of a DVL-aided INS and in the presence of water currents.

Ranges from these trajectories to the two commercial LBL transponders are plotted in figure 7. These plots support our previous observations, illustrating close agreement between the ranges output by the independent LBL acoustic system and the trajectory resulting from our piUSBL approach. Again, naive DR quickly diverges from the transponder ranges. Although the LBL system is queried by the vehicle at a rate of 0.2 Hz, only about 32% of those queries were met with a valid response (detected with power above a certain

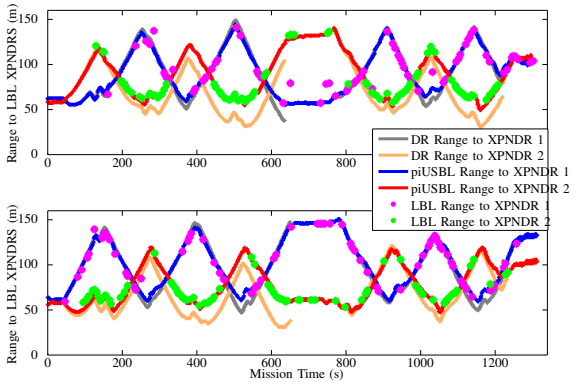

Fig. 7: Ranges to LBL transponder (XPNDR) 1 and 2 calculated from trajectory estimates - ranges to transponder 1 and 2 are: blue and red respectively for piUSBL trajectory; gray and orange respectively for dead-reckoned trajectory; and magenta and green respectively for commercial LBL raw values. *Top:* Run 1. *Bottom:* Run 2.

threshold), indicating the acoustically challenging nature of the river. As a result, an even smaller percentage ($\sim 10\%$) of LBL ranges occur concurrently for both beacons – without concurrent ranges, LBL-based localization is not possible; this is the reason why we have opted to compare piUSBL to LBL range measurements directly, rather than compare piUSBL and LBL position estimates. Outliers in the LBL ranges are apparent (e.g. in run 1 650–760 s when the vehicle is stationary while receiving GPS), but this data still allows us to validate the navigational ability of our system.

Taking the absolute difference between the ranges outputted by the trajectory estimates and the raw ranges from the LBL system allows us to plot error statistics with respect to LBL, as shown in figure 9. For run 1, piUSBL has a median error of 1.74 m, with 75% of measurements falling below 3.62 m; and for run 2, piUSBL has a median error of 2.22 m, with 75% of measurements falling below 3.90 m. The mean absolute error (MAE) for piUSBL is 3.14 m and 2.91 m for runs 1 and 2 respectively, while for DR it is 11.14 m for run 1 and 9.42 m for run 2. These results suggest that the piUSBL system significantly improves the navigational ability of the SandShark AUV.

VI. Moving Beacon Relative Navigation

A. Field Experiments

To validate the feasibility of the relative navigation operating paradigm, we performed an initial test using our SandShark AUV in Ashumet pond in Falmouth, MA. In this run, our custom acoustic beacon was manually towed by an inflatable kayak, and was set to broadcast a 20 ms, 7–9 kHz LFM up-chirp (left side of figure 2), at a depth of about 1.5 m. Custom MOOS-IvP behaviors instructed the vehicle to dive to 1.5 m and search for the beacon, home-in on it, and continuously loiter in a 12 m diameter circle around it, as the beacon was periodically repositioned.

Unfortunately in this case no LBL system was deployed, and so only the internal odometry of the AUV was available to estimate absolute AUV position. To verify that the vehicle was indeed homing in on the beacon, a forward-pointing GoPro camera was mounted to the payload, allowing us to visually confirm the beacon during flybys.

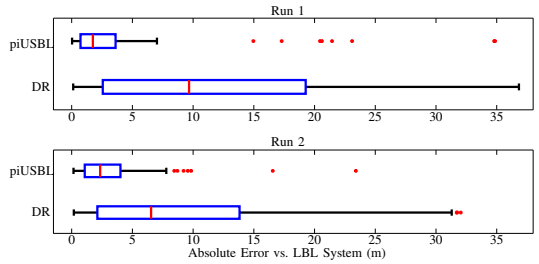

Fig. 9: Error statistics for piUSBL and dead-reckoned (DR) trajectory estimates when compared to the independent commercial LBL system.

B. Results

Figure 10 displays the dead-reckoning trajectory of the vehicle, as well as the GPS positions of the kayak/beacon. The kayak/beacon moved through three different station-keeping latitude/longitude coordinates - the first at about $(41.6346, -70.5388)$, the second at approximately $(41.6343, -70.5387)$, and the third at about $(41.6341, -70.5388)$. Although DR is fairly inaccurate, the trajectory of the vehicle is indicative of successful detection, tracking, homing, and loitering by the AUV around the beacon, while being repositioned, with three distinct loitering patterns visible. The inaccuracy of the absolute DR estimate is apparent when looking at the jump in position from a GPS update during an unexpected surfacing event at $(41.6345, -70.5387)$, as well as when the vehicle surfaced at the end of the mission.

Successful relative navigation is also supported by imagery captured from the vehicle-mounted GoPro as shown in figure 8. These images provide visual confirmation of successful beacon homing and tracking, with image timestamps that correspond well with DR trajectory positions during which the vehicle came into close proximity to the beacon.

Figure 11 illustrates plots of the estimated range and azimuth calculated from our beacon state estimate $\vec{s}^{\,llf}(t)$ of our piUSBL system, overlaid with argmaxs of the range signal and beamformer power output, calculated offline through exhaustive search. Outliers in the range and beamformer measurements are apparent, but are well rejected by the piUSBL filter. The good agreement between the argmax measurements and the filtered signal indicates that our sequential Monte-Carlo beamformer approach works well to integrate the measurements with the AUV motion model, even with a mobile beacon. Discontinuities in the piUSBL output are likely due to long periods of acoustic occlusion, during which the filter is unable to incorporate measurement updates.

VII. Conclusion and Future Work

In this paper, we have presented an acoustic approach that enables a miniature, very low-cost autonomous underwater vehicle (AUV) to navigate without the use of a DVL-aided INS. The system has two defining characteristics: the use of a single periodically broadcasting beacon, which improves usability and lowers cost; and a vehicle-mounted passive USBL array for beacon signal detection and processing, which enables scalability. Acoustic processing calculates both range and angle between the AUV and the beacon, and

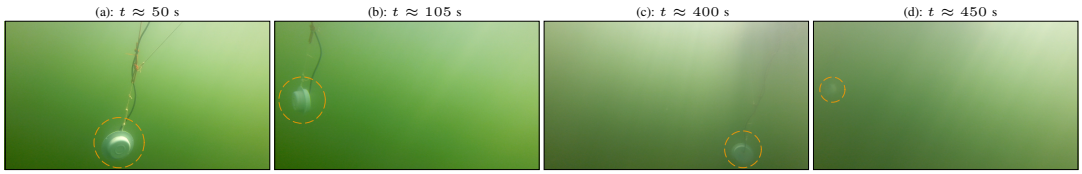

Fig. 8: Imagery of the beacon captured by a SandShark-mounted GoPro during the relative navigation beacon homing flybys - the underwater speaker of our custom acoustic beacon is highlighted by dashed orange circles. The time that each flyby occurred is listed above each image.

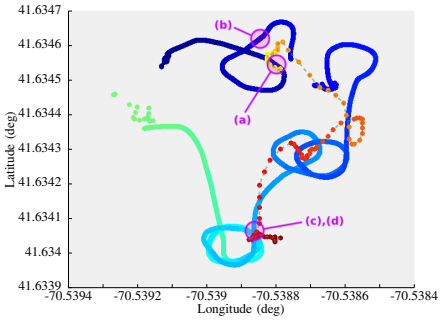

Fig. 10: SandShark dead-reckoned trajectory for relative navigation mission with beacon homing and loitering. Blue-green trajectory is AUV internal odometry, and yellow-red is kayak and beacon GPS trajectory, with gradients indicating mission time. Purple circles indicate visual confirmation of the beacon during flybys, with labels corresponding to images in figure 8.

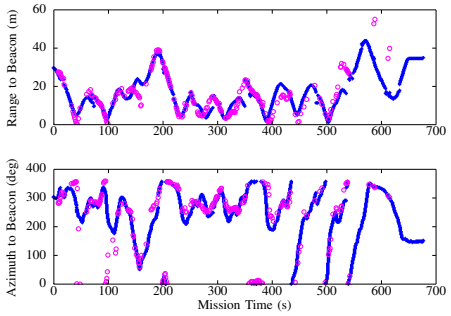

Fig. 11: Estimated relative range and azimuth from the AUV to the moving beacon - the real-time on-board piUSBL filter estimate is plotted in blue, and offline arg-maximums for range and azimuth found through exhaustive search are overlaid as magenta circles.

closed-loop navigation on a low-cost embedded computer is achieved by closely coupling beamforming and particle filtering, allowing the vehicle to fuse acoustic measurements and odometery in a computationally efficient manner. Results from closed-loop navigation experiments have demonstrated the effectiveness of the system at performing absolute navigation, with verification provided by an independent LBL system. In addition, initial results of relative navigation against a moving beacon have demonstrated the feasibility of this operating paradigm, opening a path toward multi-AUV operations over large spatial length scales.

Future work includes characterizing our system against a highly-accurate, dual-antenna GPS, allowing us to quantify the angular and range accuracy of our approach. We are also working to add a second acoustic beacon to our system, which we suspect will greatly improve localization accuracy at a modest downgrade in ease-of-use. The use of two beacons will also enable the estimation of heading without a magnetometer, which is especially useful for low-cost AUVs and ROVs that experience magnetic interference in structured environments. Finally, we are working toward replicating our system on a fleet of SandShark AUVs, which will allow us to investigate the difficulties and benefits of multi-AUV operations in the context of relative navigation.

Acknowledgments

This work was funded by ONR award number N00014-16-1-2081, Lincoln Laboratory award number PO 7000339130, and Battelle award number PO 472523.

References

[1] H. P. Tan, et al., *A Survey of Techniques and Challenges in Underwater Localization*. Ocean Engineering, vol. 38, no. 14, pp. 1663-1676, 2011.
[2] G. M. Trimble, *The Doppler Inertial Acoustic System For Littoral Navigation (DIAS)*. IEEE AUV, pp. 27-33, 1998.
[3] M. B. Larsen, *High Performance Doppler-Inertial Navigation - Experimental Results*. IEEE OCEANS, pp. 1449-1456, 2000.
[4] A. Underwood, C. Murphy, *Design of a Micro-AUV for Autonomy Development and Multi-Vehicle Systems*. IEEE OCEANS, 2017.
[5] Y. T. Tan, M. Chitre, F. Hover, *Cooperative Bathymetry-Based Localization Using Low-Cost Autonomous Underwater Vehicles*. Autonomous Robots, vol. 40, no. 7, pp. 1187-1205, 2016.
[6] J. Wang, S. Bai, B. Englot, *Underwater Localization and 3D Mapping of Submerged Structures with a Single-Beam Scanning Sonar*. IEEE ICRA, pp. 4898-4905, 2017.
[7] A. Mallios, et al., *Scan Matching SLAM in Underwater Environments*. Autonomous Robots, vol. 36, no. 3, pp. 181-198, 2014.
[8] P. Newman, J. Leonard, *Pure Range-Only Sub-Sea SLAM*. IEEE ICRA, pp. 1921-1926, 2003.
[9] J. Vaganay, et al., *Experimental Validation of the Moving Long Base-Line Navigation Concept*. IEEE AUV, pp. 59-65, 2004.
[10] J. Curcio, et al., *Experiments in Moving Baseline Navigation Using Autonomous Surface Craft*. IEEE OCEANS, 2005.
[11] S. Singh, et al., *Underwater Acoustic Navigation with the WHOI Micro-Modem*. IEEE OCEANS, 2006.
[12] J. Melo, A. Matos, *Towards LBL Positioning Systems for Multiple Vehicles*. IEEE OCEANS, 2016.
[13] B. Hodgkinson, D. Shyu, K. Mohseni, *Acoustic Source Localization System Using a Linear Arrangement of Receivers for Small Unmanned Underwater Vehicles*. IEEE OCEANS, 2012.
[14] M. Morgado, P. Oliveira, C. Silvestre, *Tightly Coupled Ultrashort Baseline and Inertial Navigation System for Underwater Vehicles: An Experimental Validation*. Journal of Field Robotics, vol. 30, no. 1, pp. 142-170, 2013.
[15] R. M. Eustice, et al., *Recent Advances in Synchronous-Clock One-Way-Travel-Time Acoustic Navigation*. IEEE OCEANS, 2006.
[16] S.E. Webster, et al., *Advances in Single-Beacon One-Way-Travel-Time Acoustic Navigation for Underwater Vehicles*. The International Journal of Robotics Research, vol. 31, pp. 935-950, 2012.
[17] B. Claus, et al., *Closed-Loop One-Way-Travel-Time Navigation Using Low-Grade Odometry for Autonomous Underwater Vehicles*. Journal of Field Robotics, pp. 1-14, 2017.
[18] N. R. Rypkema, E. M. Fischell, H. Schmidt, *One-Way Travel-Time Inverted Ultra-Short Baseline Localization for Low-Cost Autonomous Underwater Vehicles*. IEEE ICRA, pp. 4920-4926, 2017.
[19] O. A. Viquez, et al., *Design of a General Autonomy Payload for Low-Cost AUV R&D*. IEEE AUV, pp. 151-155, 2016.
[20] M. R. Benjamin, et al., *Nested Autonomy for Unmanned Marine Vehicles with MOOS-IvP*. Journal of Field Robotics, vol. 27, no. 6, pp. 834-875, 2010.
[21] H.L. Van Trees, *Optimum Array Processing*. John Wiley & Sons, 2002.